# New study of the local gravity field of El Hierro (Canary Islands)

F.G. MONTESINOS, J. ARNOSO and M. BENAVENT

Instituto de Astronomía y Geodesia (CSIC-UCM).
Facultad de Matemáticas, Plaza de Ciencias,3. 28040, Madrid, Spain.
fuensanta_gonzalez@mat.ucm.es; jose_arnoso@mat.ucm.es; mbenavent@mat.ucm.es

**ABSTRACT**
El Hierro island has been built-up at the from a classic triple armed rift system, being its subaerial morphology enhanced by large scale landsliding. The ridges are marked on the Island by frequently aligned faults and volcanic centres. Three volcanic cycles take part in its evolution: Old, Intermediate and Recent Series, which can be clearly separated. The Bouguer anomaly map in this island shows several gravity anomalies which can be associated to the different stages of its growth. A detailed study, increasing the number of gravity stations and improving previous researches, has let us establish a better interpretation of the local gravity anomalies associated with the recent volcanism in the area.
To remove the influence of the deepest sources of the gravity field in this local study, we identify a regional trend by a robust polynomial fit. The residual map is analyzed with statistical techniques. The observational noise is filtered distinguishing the signal corresponding to the local gravity field. The inversion of these data is based on a genetic algorithm which optimizes the model of distribution of gravity sources by emulating the Darwin's principle about evolution. The geometry of these sources is determined upon a prismatic partition of the subsurface, and adopting a priori values of density contrasts.
This local gravity study shows low-density bodies following the concentration of recent emission centres on El Hierro, and they conform the three-armed rift structure regularly developed in this island. The high density structures coincide where the oldest volcanism outcrops, just in the areas which suffered giant landslides.

**Keywords:** Canary Islands, gravity inversion, genetic algorithm, volcanism, optimisation method



ISSN: 0214-4557

## 1. INTRODUCTION

Gravity methods have been applied widely to investigate the structure of volcanoes, and range from detailed modelling of summit areas to determine recent eruptive history (e.g. Chandrasekhar et al. 2002) to broad scale modelling of subvolcanic intrusions (e.g. Williams & Finn 1987). Thus, to provide insights into their internal structure and postshield evolution, many gravity surveys have been undertaken on ocean island volcanoes (e.g. (Kauahikaua et al. 2000; Canales et al. 2002, Montesinos et al. 2005a, etc)

Previous geodetic and gravimetric studies that we have carried out on El Hierro island (Montesinos et al 2005b; Arnoso et al. 2005; Gorbatikov et al. 2005), give us a better understanding of its inner structure and evolution. Moreover, from other geophysical studies we can confirm several structures identified in our model of sources of gravity field (e.g., Hausen 1972; Pellicer 1977; Fuster et al. 1993; Carracedo et al. 1997; Carracedo et al. 2001).

In this work we have used new gravity data, which complete the former data set observed on the island (Montesinos et al. 2005b), reducing the distance between contiguous stations. This fact determines the minimum depth of inversion model (e.g., Fedi & Rapolla 1999) providing a more complete information of the shallower crustal structures that could be associated with recent volcanism. A regional trend in the gravity field is identified and by removing it, a residual anomaly map is obtained. The last is analysed to calculate the signal of gravity anomaly field, filtering the noise. To analyze the new gravity map, filtering the noise produced by erroneous or incomplete reductions (e.g., from an average terrain density), we applied a covariance analysis and a least squares prediction. Interpretation of this anomaly map, corrected for regional trends and filtered, provides us information on the spatial distribution of anomalous bodies that may be connected to the volcanic phenomena.

The distribution of these bodies according to their density contrasts is determined by the inversion of these gravity data. The solution to this problem is non-unique and is, moreover, limited because the data are restricted to a discrete set of inaccurate values. To deal with this issue, additional information about the model parameters (subsurface structure) and the data parameters (statistical properties of inexact data as, for instance, Gaussian distribution) are taken into account in the inversion process.

In this work, we apply our inversion technique based on a genetic algorithm (Montesinos et al. 2005a) without resorting to an interpolated grid that can alter or smooth the solution. Moreover, we complete the inversion model offshore using marine gravity data. Finally, we discuss the results obtained in this local gravity study.

## 2. GEOLOGICAL SETTING

El Hierro and La Palma (Fig. 1) are the youngest and westernmost islands of the archipelago and, along with Tenerife, seem to have been the most active in terms of volcanic and landslide activity in the recent past . Three giant lateral collapses can be seen in the onshore geology of El Hierro (Carracedo et al. 1999): the Tiñor, El Julán and El Golfo, which is the most recent massive landslide of the archipelago (Fig. 1). The San Andrés fault on the NE flank of the island may correspond to an aborted lateral collapse (Day et al. 1997) and the embayment of Las Playas, on the SE flank of the island, may be a similar feature (Fig. 1).

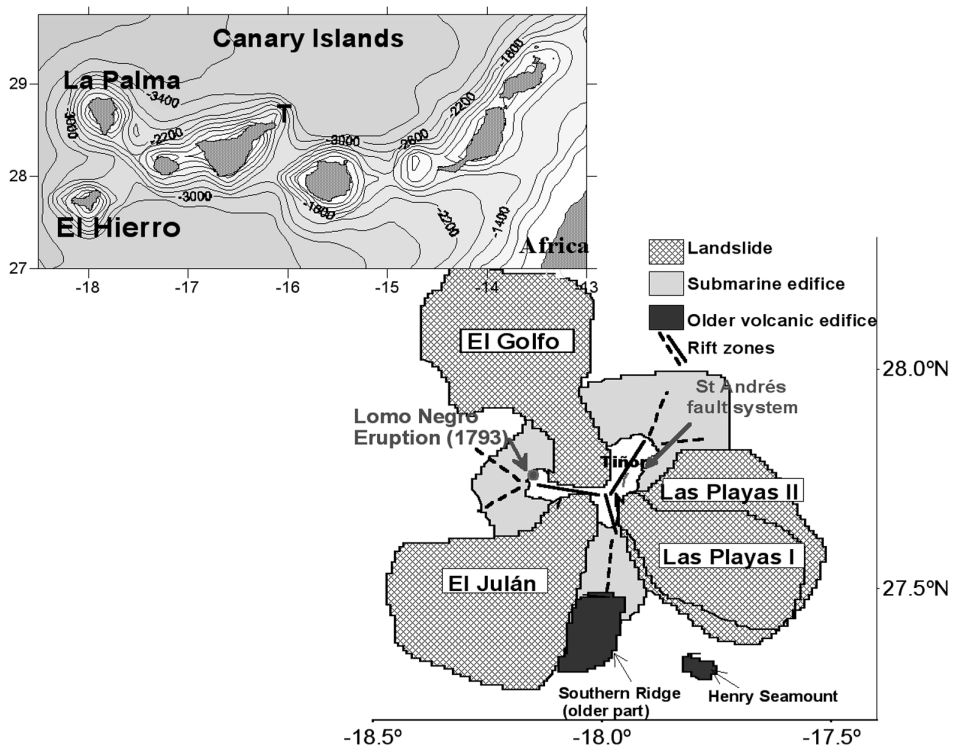


**Figure 1.** Morphological interpretation of El Hierro and surrounding submarine flanks (adapted from Gee et al. 2001). Onshore rift zones are taken from previously published geological mapping (thick black lines) and interpreted locations of offshore rift zones are shown as thick, dashed lines.

With a surface about 278 km$^2$ and a maximum altitude of 1,501 m in its central region, according to several authors (e.g., Fuster et al. 1993; Carracedo et al. 1999), El Hierro has been built up from an active Y-shaped rift, with the NE and NW branches more active than the S branch. This island was probably formed over a stationary source of magma presenting a perfect concentric development, with superimposed volcanoes and a regular three-armed rift geometry arranged at approximately 120º (Carracedo 1996). In this sense, Gee et al. (2001) suggested that rifting activity might not be confined to narrow zones and, furthermore, the Southern Ridge could be part of an older, eroded volcanic edifice that predates much of the other submarine flanks of El Hierro (Fig. 1).

El Hierro, which is still in its juvenile stage of shield growth, shows three main volcanic units associated with successive volcanic edifices and directly related to the giant landslides: a) Tiñor volcano, b) the El Golfo edifice, c) the rift volcanism. Fuster et al. (1993) distinguished three periods of activity. The Ancient series (A and B) correspond to the shield stage and they outcrop in the NE of the island, in a high area and in the walls of El Golfo, Las Playas and on the Western coast. These authors postulated the existence of a first emission period from independent edifices that remained isolated. In the beginning, they may have been joined, but were separated by destructive phenomena. The main emission centre of this edifice may be near the centre of El Golfo depression.

The intermediate and recent series (posterosional or rejuvenated stage) were established to distinguish the eruptive materials overlapping the ancient series. Some volcanic edifices of the recent series are well preserved, such as Soliman volcano (near of San Andrés). The only historic eruption could have occurred in Lomo Negro, on the Western coast of the island (Hernández-Pacheco 1982) in 1793. Thus, the rift volcanism forms a relatively thin sequence with emission vents distributed in three volcanic rift branches that have not as yet produced a topographically distinct edifice. Rifts are defined by the concentration of eruptive vents.

With respect to the the thickness of the crust, several authors have used seismic measurements and free-air anomalies to study this feature in El Hierro, estimating a Moho depth of around 15,000-16,000 m (Bosshard & MacFarlane 1970; Watts 1994).

## 3. TOPOGRAPHIC AND GRAVITY DATA. ANALYSIS OF GRAVITY ANOMALIES

The topographic data used to calculate the gravity data terrain correction are a 1:25,000 scale digital terrain model provided by the National Geographic Institute of Spain (Fig. 2), supplementing this information with ETOPO2U (National Geophysical Data Center) bathymetric data.

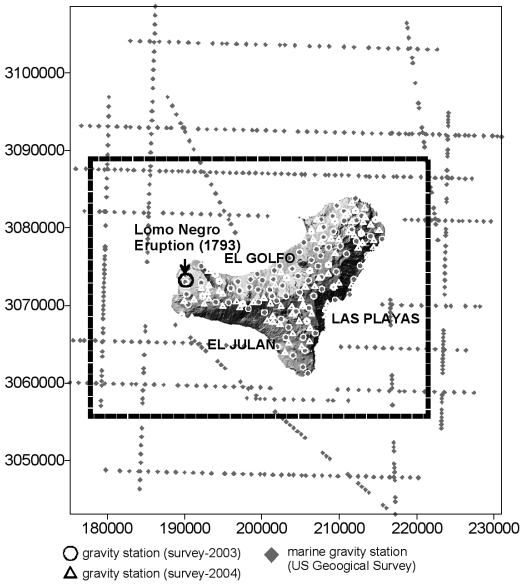


**Figure 2.** Distribution of gravity stations over the digital terrain model 1:25000 (National Geographic Institute, Spain). We performed two land gravity surveys (2003, 2004) incorporating marine gravity data from US Geological Survey (Folger et al. 1990), in order to better define the gravity map of this area. Map is referenced to UTM coordinates. The dotted rectangle shows the zone used in the analysis and inversion processes.

We consider two gravity data sets from different sources. First, the observations that we conducted in 2003 and in 2004, with a LaCoste & Romberg, model G, gravity meter with digital electronic readouts. We measured a total of 165 stations on El Hierro, with a nearly homogeneous distribution and located at average intervals of 875 m and maximum distance of 1,524 m (Fig. 2). The coordinates of the gravity stations were obtained by differential GPS observations. These gravity data were corrected with the empirical tidal model for Canarian Archipelago (Arnoso et al. 2001). Adjusting the observations of repeated data and correcting for drift, jumps and tides, produced residuals with a standard deviation of 0.020 mGal (1 mGal=$10^{-5}$ ms$^{-2}$). The second source of data used to detect the regional trend in the gravity was marine gravity data, provided by U.S. Geological Survey (USGS), collected from a cruise in 1987 aboard the Starella Research Vessel (Folger et al. 1990), up to 10,000-25,000 m offshore of the island (Fig. 2).Thus, there are 710 gravity stations in this area.

Once the data were reduced and homogenized (referred to IGSN 1971), the Bouguer anomaly was computed. In Montesinos et al. 2005b, we describe the

process to select a suitable average terrain density that reduces the gravity anomaly field distortion. We use a mean value of 2,510 kg/m$^3$ for the density of the terrain masses and a value of 1,027 kg/m$^3$ for the seawater, which is in line with the density calculated for the other islands of this archipelago. Taking into account that this value is an average density for several regions of the island, the results in the inversion process may be influenced by an excess -or deficit- of terrain correction, which will be reflected in the local gravity anomalies field.

The obtained refined Bouguer anomaly of El Hierro (Fig. 3) is dominated by maximum values onshore except on the Western and Southern edges of the island. Although the offshore prolongation of the main maximum seems to be located towards the North-Western area, this is not well defined because of the data gap near the coast. The marine gravity data indicate the Eastern area dominated by a strong gravity minimum with lowest values in the area occupied by the Las Playas landslide. These data also give minimum values in the area of El Julán landslide (see Fig. 1). However, the offshore continuation of the NW and S ridges coincides with maximum gravity values. Taking into account the long wavelength signal in the gravity map, it is possible to considerer a general tendency of increasing the gravity values from Southeastern to Northwestern zone.

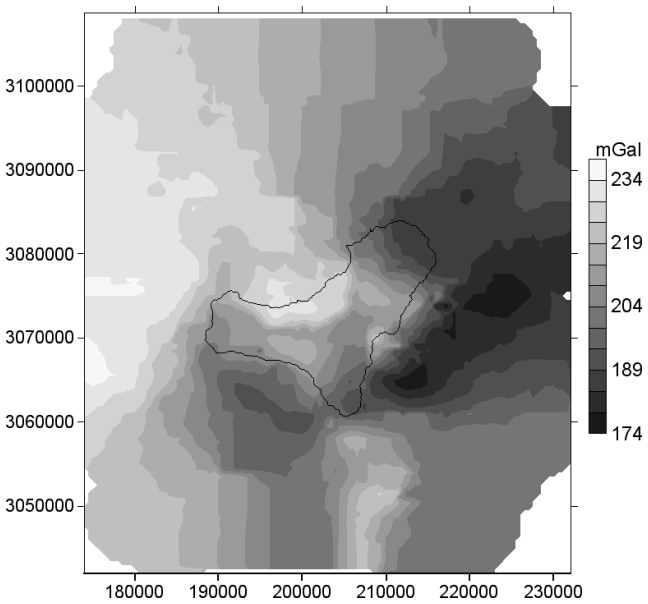


**Figure 3.** Bouguer gravity anomaly map. The density value used to correct the terrain effect is 2.51 g/cm$^3$. Contour interval is 5 mGal. A clear gravity gradient is observed from El Hierro zone towards the west. These high Bouguer anomaly values could correspond to normal oceanic lithosphere not affected by volcanism (Carbó et al. 2004).

## 4. REGIONAL COMPONENT AND ANALYSIS OF THE GRAVITY MAP

Respect to the clear gravity gradient observed from El Hierro zone towards the Northwest, these high Bouguer anomaly values could correspond to normal oceanic lithosphere not affected by volcanism (Carbó et al. 2004). In the Bouguer anomaly map, this regional trend could hide other interesting effects caused by shallow sources. For this reason, it is necessary to identify the regional trend, and to remove it from the Bouguer anomaly map. The resulting residual map will be named the local anomaly map. We identified this regional component with a polynomial surface. However, standard polynomial fitting methods pose problems of inconsistency in their formulation and produce fitted polynomials which are heavily influenced by the residual field. An interesting polynomial method that avoids the former problems for the regional gravity estimation is the robust polynomial fitting method (Beltrao et al. 1991). This method of regional-local separation is based on polynomial fitting in which the coefficients of the polynomial are determined by a robust procedure consisting of iteratively re-weighted least squares solutions. We repeated the iterative process to obtain a stable solution. For El Hierro area we selected the 2$^{nd}$ degree robust polynomial fitting as the best way of representing a simple regional trend, resulting in a residual anomaly (Fig. 4) that corresponds to local structures. The centred residual anomaly, $\Delta \mathbf{g}$, ranges from -25 to 20 mGal with a standard deviation of 8.51 mGal.

Taking into account that the aim of this work is the study of the local gravity field in El Hierro island, we can deal with an smaller area of the survey than the one that we would consider to identify the regional component. So, it is possible to reduce the number of parameters in the following process. Thus, we take the land data and the offshore data, which are next to the island, being a total of 422 data points (Fig. 2).

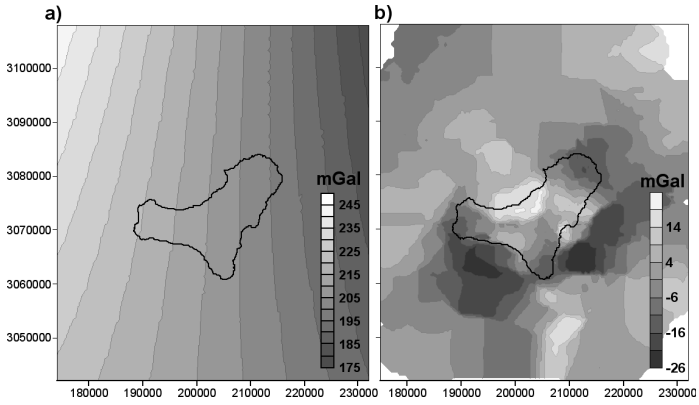


**Figure 4.** a) Regional component identified with a polynomial surface of degree 2 calculated by means of robust technique. b) Residual component obtained removing the regional component from gravity data.

The possibility of errors in the observations and in the data reductions (for example, the rugged local topography suggests some inaccuracy in the terrain correction calculated for stations close to the slopes) could produce distortions in the anomaly map. For this reason, to filter these perturbations (noise **n**) and to obtain a continuous model (signal **s**) of the autocorrelated gravity anomaly, we applied a covariance analysis and a least squares prediction (Moritz 1980). The values of these errors are calculated by means of the results of the covariance analysis and filtering process. By using a correlation analysis of the data, $\Delta\mathbf{g}$, and assuming that the covariance between two stations depends only on the horizontal distance, a distribution of empirical covariance is adjusted with a suitable analytical covariance function. A first estimation of the signal, $\hat{\mathbf{s}}_1$, at this level of covariance, and the prediction error matrix are obtained by least-squares prediction. We repeat this process to detect signals of minor amplitude in the residual values (observed data minus estimated signal). This procedure ends when no further signal can be identified. From these estimated signals, the distribution of the resulting residuals displays the non-correlated noise, **n**. So, we adopted the following decomposition for the local gravity data,

$$\Delta\mathbf{g} = \hat{\mathbf{s}} + \mathbf{n}$$

where $\hat{\mathbf{s}}$ represents the map of the local anomaly model, obtained by adding the successive estimated signals.

Performing the covariance analysis of the residual gravity map of El Hierro, two levels of correlated signal have been detected. With two successive approaches, firstly over the residual map (data minus regional component) and, secondly, over the residual minus previous estimated signal, the successive correlation analysis of the data gave us a distribution of empirical covariances, which were adjusted by means of suitable analytical covariance functions (Fig. 5). Using these covariance functions, the usual formulae for least squares prediction (Moritz 1980) gave us two predicted signals. Adding these signal we obtained the local gravity signal, filtered of uncorrelated part of the data corresponding to the noise. In Fig. 5, we show the distribution of this non-correlated noise (the resulting residual values). The standard deviation of this final noise **n** is about 0.512 mGal, which corresponds mainly to errors on data after correction for local terrain and erroneous elevation data.

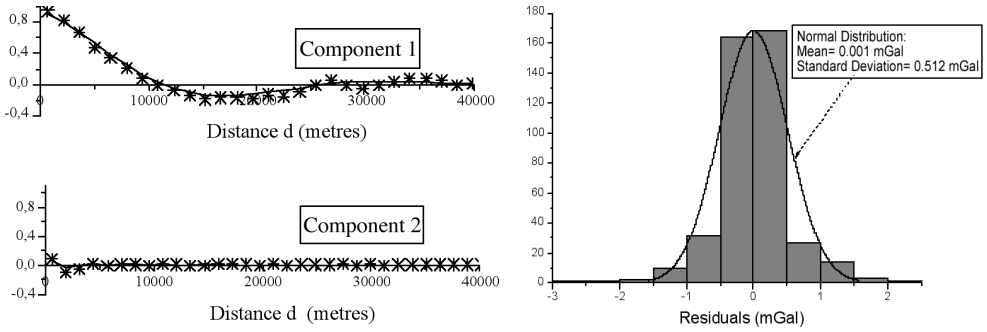


**Figure 5.** Covariance functions adjusted (line) to the two successive empirical covariance distributions (stars). The analysis of the residual map of gravity anomaly is achieved on the area marked in Fig. 2. Histogram of the residuals of the filtering process. This non-correlated noise of the data follows a normal distribution of mean -0.001 mGal and standard deviation 0.512 mGal.

The signal estimated represents the detected gravimetric effect of the shallower subsurface structures. These will correspond to anomalous bodies located between sea level and some 6,000 m depth.

## 5. GRAVITY INVERSION

To interpret the geometry and location of the sources of these anomalies, the local anomaly map is inverted using a general 3-D inversion scheme applying the method proposed in Montesinos et al. (2005a). The 3D gravity inversion is based on genetic algorithms (GA), aiming to determine the geometry of the sources of the observed gravity field, upon a prismatic partition of the subsoil volume, and adopting a priori density contrast values.

GA consists of search methods modeled on the evolutionary behavior of biological systems, according to Darwin's evolution principle. Following the GA principles, we put forward the gravity inversion problem as an evolutionary process where the individuals are the possible models (prismatic partition) that represent the sources of the observed gravity anomaly field (anomalous bodies). This inversion approach seeks the geometry of the sources of the gravity field, adopting the hypothesis that these structures are characterized by $q$ prescribed mass density contrasts, $\boldsymbol{d}=\{d_1,...,d_q\}$. Thus, the anomalous sources are constructed by assigning to each prism one of the $q$ prescribed density contrasts. In this case, our GA works over a set of models (a population of individuals), making successive modifications in an iterative process, seeking a model that minimizes the discrepancy between the gravity field generated by the model and the

observed gravity data (error function). The model parameters are the densities of each prism of each individual of the population.

Let us consider $n$ gravity stations $P_i(x_i,y_i,z_i)$, $i$=1,..,$n$, not necessarily gridded, located in a rugged topography and with observed gravity anomaly values $\boldsymbol{g}_{obs}$. The element $A_{ij}$ of the matrix $\boldsymbol{A}$ corresponds to the gravity attraction, at the $i$-th station $P_i(x_i,y_i,z_i)$, due to the $j$-th prism, for unity density. The gravity anomaly in the $i$-th station $P_i$, $i$=1,...$n$, produced by the model $\boldsymbol{m}_k$ is

$$g_i^k = \sum_{j=1}^{m} A_{ij}\, \rho_j^k \,. \qquad (1)$$

We define the error function, which must be minimized and determines the adjustment of each individual by (Montesinos et al. 2005a) as

$$F(\boldsymbol{m}_k)=\left(\boldsymbol{A}\boldsymbol{m}_k - \boldsymbol{g}_{obs} - \boldsymbol{G}_m\boldsymbol{u}\right)^{\mathrm{T}} \boldsymbol{E}_{ss}^{-1} \left(\boldsymbol{A}\boldsymbol{m}_k - \boldsymbol{g}_{obs} - \boldsymbol{G}_m\boldsymbol{u}\right) + \beta\, \boldsymbol{m}_k^{T}\boldsymbol{C}_M\boldsymbol{m}_k \;, \quad (2)$$

where $\boldsymbol{u}$ is an unitary vector, $b$ is an empirically determined parameter corresponding to the Tikhonov regularization technique (Schwarz 1979), and the $m$x$m$ matrix $\boldsymbol{C}_M$ describes the uncertainty of the model. This matrix is diagonal and its elements are defined by the inverse of the diagonal elements of $\boldsymbol{A}^{\mathrm{T}}\boldsymbol{E}_{ss}\boldsymbol{A}$. So, we assign a value relative to the gravity attraction that it produces at the stations to each prism, defining in this way its uncertainty. The data error matrix $\boldsymbol{E}_{ss}$ can be obtained from previous covariance analysis (Moritz 1980).

The process starts with a population of $np$ models, $P(0)$, which can be generated randomly or, to avoid premature convergence to a non-suitable model, it can be started with all models identical, without information, where all the prisms have null density contrasts (empty models).

The size of the population, $np$, is selected as a function of the quantity of prisms, data, etc., (generally a value of 10 gives successful results, although another selection would not alter the results but instead the convergence rate) and is invariant throughout the process. In the iterative procedure, the individuals of the population are evaluated (error function (2)) and can be chosen (selection operator) to continue the evolutive process. Then, two genetic operators (mutation and cross) act on these selected models producing $l$ new individuals, which are also evaluated. Then, the selection operator chooses, from these $np + l$ (new) models, the best $np$ individuals, and the iterative procedure is repeated.

The selection operator (Michalewicz 1994) acts according to a cumulative probability defined from the error function. To create new models, the mutation and crossover operators act on these selected individuals. The mutation provides random diversity in the population according to a predefined probability $p_m$, changing some prisms of some models. The next operator, crossover, acts over

selected models with probability $p_c$. The models selected to cross exchanges the distribution of density values of their prism from the position selected at random. In Montesinos et al. (2005a) we explain with detail these operators. Although most authors (e.g., Michalewicz 1994) choose very low mutation rate values (about 0.01), because they usually work with few unknowns, we suggest a value of $p_m$ =0.3 (this value can be increased if the amount of unknowns increases). Respect to crossover rate, we use a value, $p_c$, of about 0.6, as is recommended in GA literature.

The modified models are evaluated again with the unmodified ones, repeating the evolutionary process (selection/mutation/crossover) until a model that minimizes the error function is found. After numerous generations, GA convergence slows greatly. In order to establish an end at this stage of the process, we introduce a predetermined value according to the accuracy of the data. The following stage consists of obtaining a plausible model, as a solution to the inverse problem, which agrees with the geological reality.

To produce a model with a smoother geometry so as to remove this uncertainty and avoid local minima, we employ a smoothing technique equivalent to minimizing the whole anomalous mass (Montesinos et al. 2005a). This operator acts in each model, when the error function is minimized, assigning each prism an averaged value of the density contrasts of the adjacent prisms. Then, these smoothed new individuals are evaluated again. If the best model fits the observed gravity data successfully according to the predefined limit, or does not improve the previous models after several stages, the inversion ends; otherwise, the evolutive process continues.

To apply this methodology in El Hierro island, taking into account that contiguous stations are some 875 m apart and the mean diameter of the survey is about 35,000 m (and the computer limitations), we partitioned the local subsurface into 14,729 rectangular prisms, with sides ranging from 800 m for the shallow elements to 1,200 m for the deepest blocks. According to the suggested method, we selected for the whole subsurface volume, the possible density contrasts by means of the extreme values -300 kg $m^{-3}$ and +300 kg $m^{-3}$, and an exponential variation law of contrasts. These values have been selected empirically to obtain connected and well-developed volumes, and they are coherent with the usual contrasts among structural elements of the Canarian volcanism. When different density contrasts are used, the resulting solutions are rather similar, although for higher contrasts, smaller volumes would be obtained.

The adjusted local model of density contrasts is shown in several horizontal sections, to several depths with respect to the sea level (Fig. 6). Some interesting features can be highlighted from this model with a view to the correlation with the geological and volcanic information. The residuals of this inversion adjustment follow a Normal distribution with a standard deviation of 0.722 mGal. In this case, we stopped the evolution process when the fit of the best model at that stage failed to improve after applying two successive smooth operators.

## 6. RESULTS AND DISCUSSION

The model obtained by means of inversion (Fig. 6) shows the distribution of the sources of the local gravity field. Therefore, our aim is the interpretation of the shallowest sections of this model. The distance between contiguous gravity stations (some 900 m) determines the minimum depth of the inversion model (e.g., Fedi & Rapolla 1999). Due to the fact that the stations are considered in their original position on the topographic surface, which is 1,500 m high in the central zone, we can consider sections from nearly 500 m.

In these shallowest sections of density contrasts, alignments of low-density bodies can be identified following the triple armed rift referenced by several authors. These alignments (NW, NE and South of the island, see Fig 6) are now more clearly seen than in the previous work (Montesinos et al. 2005b) and are justified by the concentration of recent (Quaternary) eruptive vents and the associated relatively recent fractures.

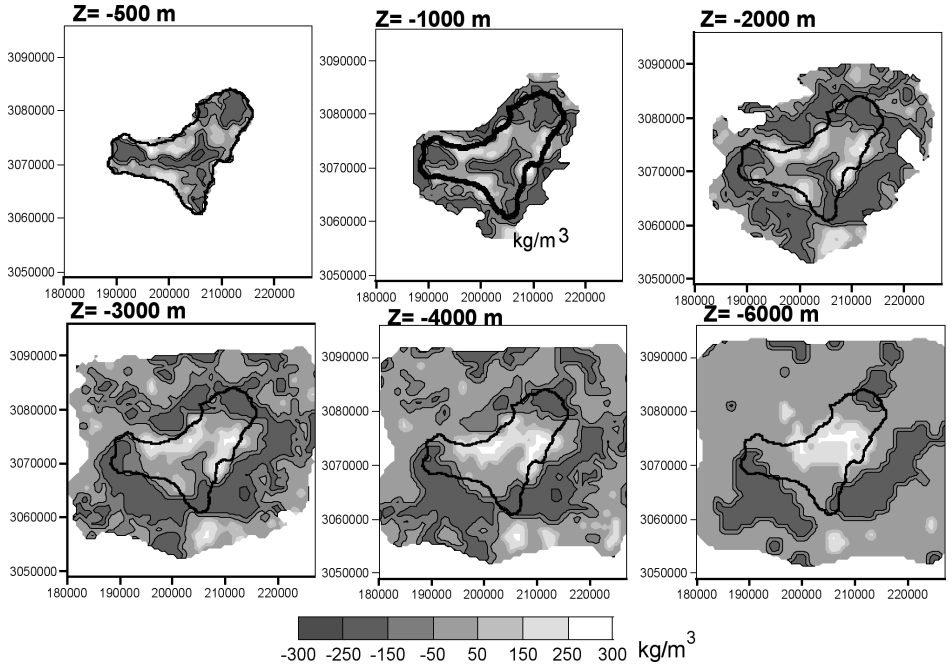


**Figure 6.** Adjusted model of density contrasts obtained by means of 3-D gravity inversion. The fixed density contrast values in the model are a discrete set of values between –300 and 300 kg $m^{-3}$. Several horizontal sections, from 500 to 6,000 m depth, are shown. At greater depths the model does not shows any structure because of removing of regional component.

The minimum density alignments on the NW, NE and South edges of the island are located in the same place as the Recent Series activity (e.g., Fuster et al. 1993). The Western coast of the island, where the single historic eruption from the Lomo Negro vent took place in 1793, is characterized by negative density contrast relative to surrounding areas (Figs. 1 and 6).

There are several high-density bodies at depths between 500 and 4,000 m that appear as independent structures at shallower sections, and join together as they go deeper. Taking into account that this model only shows the sources of local gravity field, the deeper sections do not display the whole information. The high density material lies near the zones where the oldest volcanism outcrops (Fuster et al. 1993) related to the Tiñor and the El Golfo volcanoes. This agrees with the fact that the present outcrops of the first volcano are confined to the NE flank of the island and inside the Las Playas embayment and the El Golfo volcano (Carracedo et al. 1999). These bodies are isolated in the area where an abundance of intrusive basaltic dykes exists (Carracedo et al. 2001). However, it could be also conditioned by the rift system and the recent volcanism that took place over the volcanic rift arms.

The structures located in the offshore areas of the model must be interpreted with caution because they are not supported by much data, a clear border effect exists and this is a local study of the gravity field. At the South of the model, a high-density body is related clearly to the eroded volcanic edifice associated by Gee et al. (2001) with the Southern ridge. In accordance with the hypothesis of these authors, this body is independent of the rest of the island.

It is remarkable that the areas occupied by landslides correspond to low-density material in these shallow sections. However there is distinction between the landslides of El Golfo and El Julán and Las Playas. In these two last areas (El Julán and Las Playas) the gravity field corresponds to deep low density sources, whereas El Golfo is associated to this type of body in shallower depths. These differences were widely studied in the previous work (Montesinos et al. 2005b)

## 6. ACKNOWLEDGEMENTS

This study was funded by the Project REN2002-00544/RIES (Spanish Ministry of Science and Technology). One of the authors (J. Arnoso) is supported by the program I3P of the European Social Fund.

## 7. REFERENCES

ARNOSO, J., FERNÁNDEZ, J., VIEIRA, R., 2001. Interpretation of tidal gravity anomalies in Lanzarote, Canary Islands. *J. Geodyn.* 31(4), 341-354.

ARNOSO, M. BENAVENT, R. VIEIRA, A.P. VENEDIKOV, 2005. First results of continuous ground tilt measurements in El Hierro island (Canarian

Archipelago). SAL2005 Workshop on Ocean island Volcanism, Sal Island, Cape Verde, 1-9 April 2005.

BELTRAO, J.F., SILVA, J.B.C. and COSTA, J.C., 1991. Robust polynomial fitting method for regional gravity estimation. *Geophysics*, 56: 80-89.

BOSSHARD, E., MACFARLANE, D.J., 1970. Crustal structure of the Western Canary Islands from seismic refraction and gravity data. *J. Geophys. Res.* 75, 4901_4918.

CANALES, J.P., G. ITO, R.S. DETRICK, and J. SINTON, 2002. Crustal thickness along the western Galápagos Spreading Center and the compensation of the Galápagos hotspot swell, *Earth Planet. Sci. Lett.*, 203 (1), 311-327

CARBO, A. MUÑOZ-MARTıN, P. LLANES, J. ALVAREZ & EEZ WORKING GROUP, 2004, Gravity analysis offshore the Canary Islands from a systematic survey *Marine Geophysical Researches* 0: 1–11(in press)

CARRACEDO, J.C., 1996. Morphological and structural evolution of the western Canary Islands: hotspot-induced three-armed rifts or regional tectonic trends?. *J. Volcanol. Geotherm. Res.* 72, 151_162

CARRACEDO, J.C., BADIOLA, E.R., GUILLOU, H., DE LA NUEZ, J., PÉREZ TORRADO, F.J., 2001. Geology and volcanology of La Palma and El Hierro, Western Canaries. *Estudios Geol.* 57 (5-6), 175-273.

CARRACEDO, J.C., DAY, S.J., GILLOU, H., TOTTADO, F.J., 1999. Giant quaternary landslides in the evolution of La Palma and El Hierro, Canary Islands, *J. Volcanol. Geotherm. Res.,* 94, 169-190.

CARRACEDO, J.C., DAY, S.J., GUILLOU, H., PÉREZ TORRADO, F.J., 1997. El Hierro, Geological excursion guidebook. International Workshop on Volcanism and Volcanic Hazards in Immature Interplate Oceanic Islands. La Palma, Canarias, Spain, 1-43.

CHANDRASEKHAR, D.V., D.C. MISHRA, G.V.S.P. RAO and J.M. RAO, 2002, Gravity and magnetic signatures of volcanic pipes of Saurashtra, India and their bulk physical properties vis-à-vis paleomagnetic and geochemical studies of exposed rocks. *Earth Planet. Sci. Lett.* 201, 277-292

DAY, S.J., CARRACEDO, J.C., GUILLOU, H., 1997. Age and geometry of an aborted rift flank collapse: the San Andrés fault, El Hierro, Canary Islands. *Geol. Mag.* 134, 523-537

FEDI M., RAPOLLA, A., 1999. 3-D Inversion of gravity and magnetic data with depth resolution *Geophysics,* 64 (2), 452-460.

FOLGER, D.W., MCCULLOUGH, J.R., IRWIN, B. J., DODD, J.E., STRAHLE, W.J., POLLONI, C.F., BOUSE, R.M., 1990. Map showing free-air gravity anomalies around the Canary Islands, Spain, Miscellaneous Field Studies Map, MF-2098-B, p. (1 sheet), U.S. Geol. Surv., United States.

FUSTER J.M., HERNÁN. F., CEDRERO, A., COELLO, J., CANTAGREL, J.M., ANCOCHEA, E., IBARROLA, E., 1993. Geocronología de la Isla de El Hierro (Islas Canarias). *Bol. R. Soc. Esp. Hist. Nat. (sec. Geol.)* 88 (1-4), 85-97.

GEE, M.J.R., MASSON, D.G., WATTS, A.B., MITCHELL, N.C., 2001. Offshore continuation of volcanic rift zones, El Hierro, Canary Islands. *J. Volcanol. Geotherm. Res.* 105, 107-119.

GORBATIKOV, A.V. J. ARNOSO, A.V. KALININA, F.G. MONTESINOS, M. BENAVENT, 2005. The El Hierro island (Canaries) model refinement on base of microseismic sounding application results. SAL2005 Workshop on Ocean Island Volcanism. Isla de Sal, Cabo Verde.

HAUSEN, H., 1972. Outlines of the Geology of El Hierro. *Commentationes Physico-Mathematicae* 43, 5-148.

HERNÁNDEZ-PACHECO, A., 1982. Sobre una posible erupción en 1793 en la isla de El Hierro (Canarias), *Estud. Geol.*, 38, 15-25.

KAUAHIKAUA, J. HILDENBRAND, T., WEBRING, M., 2000. Deep magmatic structures of Hawaiian volcanoes, imaged by three-dimensional gravity models. *Geology.* 28 (10), 883–886.

MICHALEWICZ, Z. 1994. *Genetic algorithms + Data structures = Evolution programs.* Springer- Verlag, Berlin, second extended edition, 340 pp

MONTESINOS, F.G. ARNOSO, J. BENAVENT, M. VIEIRA, R., 2005b. The crustal structure of El Hierro (Canary Islands) from 3-d gravity inversion. *Journal of Volcanology and Geothermal Research* (in press)

MONTESINOS, F.G.; ARNOSO, J.; VIEIRA, R., 2005a. Using a genetic algorithm for 3-D inversion of gravity data in Fuerteventura (Canary Islands), *Int. J. Earth Sci.* 94, 301-316

MORITZ, H., 1980. *Advanced Physical Geodesy.* Herbert Wichmann Verlag, Karlsruhe, Germany: 500 pp.

PELLICER, M.J., 1977. Estudio volcanológico de la Isla de El Hierro (Islas Canarias). *Estud. Geol.*, 33, 181-197.

SCHWARZ K.P. (1979). Geodetic improperly posed problems and their regularization. *Bolletino di Geodesia e Scienze Affini* 3: 389-416

WATTS, A.B., 1994. Crustal structure, gravity anomalies and flexure of lithosphere in the vicinity of the Canary Islands. *Geophys. J. Int.* 119, 648-666.

WILLIAMS, D.L. and FINN, C., 1987. Evidence for a shallow pluton beneath the goat rocks wilderness, Washington, from gravity an magnetic data. *J. Geophys. Res*. 92: no. B6, 4867-4880.